Geophysical Research Letters

RESEARCH LETTER
10.1029/2022GL100975

Dry Live Fuels Increase the Likelihood of Lightning-Caused Fires

Krishna Rao[1], A. Park Williams[2], Noah S. Diffenbaugh[1,3], Marta Yebra[4,5], Colleen Bryant[4], and Alexandra G. Konings[1,3]

[1]Department of Earth System Science, Stanford University, Stanford, CA, USA, [2]Department of Geography, University of California, Los Angeles, Los Angeles, CA, USA, [3]Doerr School of Sustainability, Stanford University, Stanford, CA, USA, [4]Fenner School of Environment & Society, The Australian National University, Acton, ACT, Australia, [5]School of Engineering, The Australian National University, Acton, ACT, Australia

Key Points:

- We provide a causal inference framework to understand the contribution of natural drivers to wildfire occurrence
- When live fuels are extremely flammable, lightning strikes are about twice as likely to cause wildfires
- The increase in fire likelihood is highest in shrubs and lowest in grass

Supporting Information:

Supporting Information may be found in the online version of this article.

Correspondence to:

K. Rao,
kkrao@stanford.edu

Citation:

Rao, K., Williams, A. P., Diffenbaugh, N. S., Yebra, M., Bryant, C., & Konings, A. G. (2023). Dry live fuels increase the likelihood of lightning-caused fires. *Geophysical Research Letters*, *50*, e2022GL100975. https://doi.org/10.1029/2022GL100975

Received 19 DEC 2022
Accepted 27 JUN 2023

Abstract Live fuel moisture content (LFMC) is a key determinant of landscape ignition potential, but quantitative estimates of its effects on wildfire are lacking. We present a causal inference framework to isolate the effect of LFMC from other drivers like fuel type, fuel amount, and meteorology. We show that in California when LFMC is below a critical flammability threshold, the likelihood of fires is 1.8 times as high statewide (2.25% vs. 1.27%) and 2.5 times as high in shrubs, compared to when LFMC is greater than the threshold. This risk ratio is >2 times when LFMC is 10% less than the threshold. Between 2016 and 2021, the risk ratio was highest in 2020 (2.3 times), potentially contributing to the record-breaking wildfire activity in 2020. Our estimates can inform several wildfire prediction and management applications, including wildfire suppression, prescribed burn planning, and public safety power shutoff implementation.

Plain Language Summary Wildfires are complex phenomena and can occur under a range of conditions, making it difficult to determine how different drivers affect wildfire occurrence. For example, dense contiguous vegetation, dry litter, dry vegetation, high winds, and warm air all contribute to high fire likelihood. Under such co-occurring conditions, how can we determine each driver's effect on fire likelihood? Here, we present a framework to attribute an individual driver's effect on fire occurrence, while controlling for other correlated factors that might provide a false signal. We consider lightning-based ignitions, assuming they are randomly distributed, and compare the fire outcomes for different vegetation dryness levels, all else held constant. We test our framework in California and find that when vegetation is dryer than the critical flammability threshold, wildfire likelihood increases by almost a factor of two. These results help clarify the uncertainty in the effect of vegetation dryness on fire occurrence, and may also help improve wildfire preparedness, management, and response strategies.

1. Introduction

Wildfire size and frequency have recently increased in the western United States (Iglesias et al., 2022), with further increases expected in the future (Abatzoglou et al., 2021; Ellis et al., 2021). Recent years have been particularly severe, with considerable impacts on ecosystems, nearby populations, and air quality. For instance, in California, wildfire burned area in 2020 was approximately double the previous record, and the eight largest fires in California's recorded history have occurred since 2017 (Cal Fire, 2021). Understanding the precise causes of these intensifying effects is challenged by the fact that wildfires are complex phenomena driven by many factors. For example, vegetation density (Hessilt, 2022), dead fuel moisture (Dorph et al., 2022), winds (Keeley & Syphard, 2019; Kolden & Abatzoglou, 2018), and extreme fire weather (Goss et al., 2020; He et al., 2022) all affect fire likelihood in complex and non-linear ways.

A first step toward understanding wildfire behavior is being able to predict its occurrence. Among the drivers of wildfire occurrence, arguably the least understood is live fuel moisture content (LFMC, the mass of vegetation moisture per unit of dry biomass). LFMC depends on not just recent hydrometeorology, but also soil and plant characteristics that affect rates of water uptake and water loss, including soil hydraulic properties, rooting characteristics, and xylem and stomatal traits (Nolan et al., 2022; Pivovaroff et al., 2019; Rao et al., 2022). Spatial variations of these traits are known to be large and likely important to LFMC and fire, but are poorly mapped (Novick et al., 2022). Furthermore, in situ LFMC measurements are prohibitively labor-intensive to be made

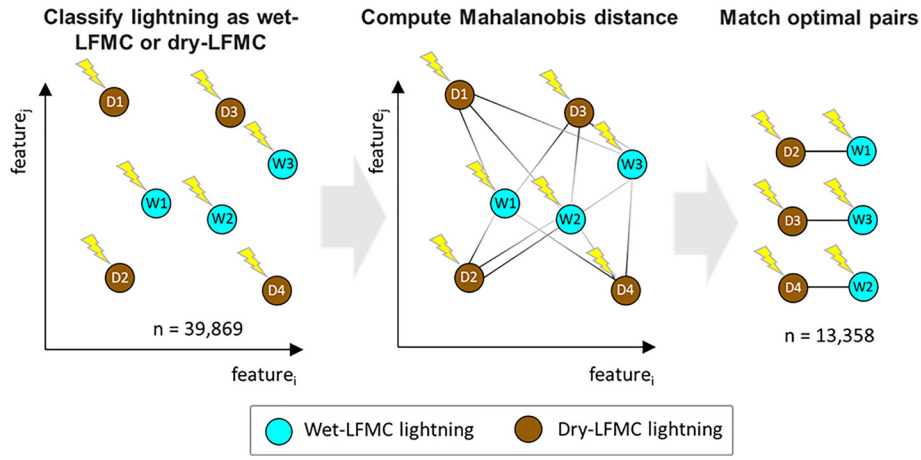

Figure 1. *Approach to select lightning events used for causal inference*. Brown (cyan) circles indicate lightning events at places where live fuel moisture content is less (greater) than a pre-determined threshold. To find matched pairs of lightning events with similar covariates, we compute the Mahalanobis distance (calculated over all covariates) across all possible dry-LFMC and wet-LFMC pairs and matched pairs were chosen to minimize the sum of the between-pair Mahalanobis distance across all matched pairs. Note that while 12 features are used for matching, only two feature axes are shown here for visualization.

at high spatio-temporal resolution. As a result, many fire danger models at most only partially account for the effects of soil and plant traits on LFMC (Bradshaw et al., 1984; Fujioka et al., 2008; Hardy & Hardy, 2007; Yebra et al., 2013). It is thus crucial to understand whether these modeling limitations significantly affect wildfire predictions.

Recent developments in remote sensing-based LFMC mapping (Quan et al., 2021; Rao et al., 2020) now enable detailed studies of LFMC's role in wildfire occurrence. Several studies show a strong threshold-like correlation between low LFMC and wildfire occurrence (Chuvieco et al., 2009; Jurdao et al., 2012; Luo et al., 2019) or burned area (Dennison et al., 2008; Nolan et al., 2016). However, correlative studies such as these may inflate the effect of LFMC on wildfire occurrence due to cross-correlation between LFMC and other wildfire drivers like atmospheric aridity and winds. Additionally, previous studies of LFMC's influence on fire occurrence have generally lacked a reliable counterfactual. For example, if a region didn't burn, was it due to LFMC being too wet, a lack of ignition sources, or other, non-LFMC-related differences with regions that did burn?

Existing studies use two methods to approximate this alternative. Some use a random sampling of all unburned areas as a comparison (Chang et al., 2013; Chuvieco et al., 2009), thereby implicitly assuming that the unburned areas also experienced an ignition, an assumption which may not always hold (Abdollahi et al., 2019; Villarreal et al., 2022). Other studies use the areas just outside the burn scar as a comparison, assuming that LFMC was too wet outside the burn scar for the burn scar to extend further (Jurdao et al., 2012; Yebra et al., 2018). Although this method has the benefit of relying on areas near known ignitions (which may have similar fuel distribution as adjacent burned areas), factors such as human containment and meteorology may also affect the shape of the burned scar, undermining the resulting inferred LFMC effects. Our solution is to focus on lightning-caused fires, taking advantage of the fact that lightning occurrence is both an observable and pseudo-random source of potential ignitions enabling robust causal inference.

2. Methods

We design a randomized control experiment to estimate the effect of LFMC on lightning ignition probability holding all other geographic, topographic, meteorological, and fuel factors constant. We create lightning pairs within land cover types with one having dry LFMC and another having wet LFMC while minimizing differences in other covariates (Figure 1). We apply our approach to forests, shrubs, and grasses in California between 2016 and 2021.

2.1. Creating Matched Pairs of Lightning Events

We classify each lightning event as occurring over either dry or wet pre-fire LFMC based on land cover-specific thresholds, with dry-LFMC lightning events defined as those associated with a pre-fire LFMC below 55% for

grasslands, below 106% for shrublands, or below 81% for forests. We choose these thresholds because previous work in Argentina showed that fire size varies across these breakpoints (Argañaraz et al., 2018), which are similar to thresholds established in Californian chaparral (Dennison & Moritz, 2009). We classify LFMC to enable causal estimation of LFMC's effect on fire likelihood based on the potential outcomes framework (see Text S1 in Supporting Information S1). However, the relevance of such thresholds may be context-specific (Pimont et al., 2019). We therefore also test the sensitivity of our results to varying degrees of LFMC difference from this threshold.

Each lightning pair consists of a dry-LFMC strike and a wet-LFMC strike, with land cover being identical and all other wildfire-related properties being as similar as possible. As covariates, we consider latitude and longitude, above-ground biomass (AGB) and dead biomass to control for fuel availability (Hessilt, 2022; Safford et al., 2022), wind speed on the lightning day (Goss et al., 2020), cumulative precipitation 12 months before the lightning day, average vapor pressure deficit (VPD) over the 4 months before the lightning day to control for soil moisture (Dadap et al., 2019), and litter moisture effects (Dorph et al., 2022) (Table S1 in Supporting Information S1). We use lagged aggregates for precipitation and VPD rather than instantaneous values because soil moisture and litter moisture have memory (McColl et al., 2017).

We control for dead fuels by replicating the Safford et al. (2022) approach to estimate dead biomass. We use annual tree mortality maps from the aerial detection and monitoring program (USFS, 2017) from 2012 to 2016, when drought-induced tree mortality was high across California (Lund et al., 2018). We filter out background mortality (shapefiles with <1 dead tree per acre) to isolate areas with recent mortality. We then create a cumulative map by summing the remaining dead trees across 2012–2016, resulting in a map with the number of dead trees at the end of 2016, the starting year of our analysis. We also use mean canopy height, its spatial variance, and the spatial variance of normalized difference vegetation index (NDVI) in the lightning pixel to control for vegetation structure and its sub-grid scale heterogeneity (Fernández-Guisuraga et al., 2021), and elevation and slope to control for topographic influences (Holden & Jolly, 2011).

To find the lightning strike pairs with the most comparable covariates, we perform a global optimization to minimize the sum of Mahalanobis distances between each pair's covariates (Text S1 in Supporting Information S1). We restrict our analysis to the peak fire period (June to November, Westerling et al., 2006) and to the period when LFMC data are available (2016–2021).

2.2. Estimating the Average Effect of Dry LFMC

The resultant data set has pairs of lightning events, each with a dry-LFMC strike and a wet-LFMC strike from the same land cover, and other similar covariates. For each pair, we analyze whether lightning ignited a wildfire in either member. We do so by checking whether a burned fire pixel appeared within 2 days of the lightning date in the lightning grid cell, which allows for errors in the detection date of a fire. This way, we label each lightning event as "fire" or "no fire." As an independent check on the accuracy of our labels, we compare our labeled fires to fires from the CAL FIRE's Fire and Resource Assessment Program (FRAP) (CAL FIRE, 2023). The FRAP investigates the causes behind select fires. Only 3.1% of FRAP fires caused by something other than lightning (covering 6% by area) are considered lightning-caused fires in our data set, adding confidence to our method. We calculate the likelihood of a fire for the dry-LFMC and wet-LFMC lightning events separately and divide the two to obtain the risk ratio (Equations 1 and 2). The risk ratio quantifies the effect of dry LFMC on the likelihood of fire relative to that of wet LFMC.

$$\text{Risk ratio} = \frac{\text{True positives}}{\text{Predicted positives}} \times \frac{\text{Predicted negatives}}{\text{False negatives}} \tag{1}$$

$$= \frac{\text{Dry} - \text{LFMC lightning with ignition}}{\text{Dry} - \text{LFMC lightning strikes}} \times \frac{\text{Wet} - \text{LFMC lightning strikes}}{\text{Wet} - \text{LFMC lightning with ignition}} \tag{2}$$

To further characterize the effects of LFMC, we re-compute the risk ratio separately for lightning events: (a) in each land cover type, (b) belonging to four equal-sized bins of LFMC difference between the two lightning events of each pair, and (c) in each year. Finally, we quantify the uncertainty associated with each estimate of the risk ratio by running a conditional maximum likelihood estimation (Fisher) test to obtain 95% confidence intervals.

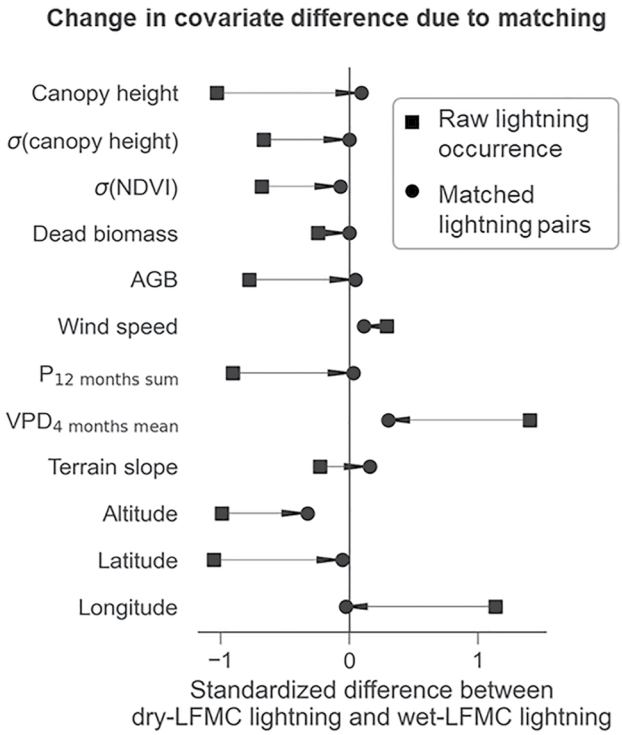

Figure 2. *Effects of matching lightning strikes on covariates*. Standardized differences in covariates before (squares) and after (circles) matching of dry-Live fuel moisture content (LFMC) and wet-LFMC lightning strikes. Lower absolute standardized differences indicate lower differences between covariates, limiting their ability to confound our inference. The σ symbol represents spatial variance within the lightning pixel (10 × 10 km).

2.3. Data Sets

We use daily lightning data from the National Lightning Detection Network (Orville et al., 2011), which has a spatial accuracy of 0.1° (~10 × 10 km). We obtain fire occurrence data from the Moderate Resolution Imaging Spectroradiometer (MODIS) burned area product MCD64A1 (Boschetti et al., 2013) at 500 m resolution. To classify lightning into dry-LFMC lightning and wet-LFMC lightning, we use LFMC mapped across the western United States at 250 m resolution and a 15-day timescale (Rao et al., 2020, Figure S1 in Supporting Information S1). These maps were created using a recurrent neural network based on synthetic aperture radar data (along with optical reflectance, topographic, and soil characteristics) and trained on ground measurements from the National Fuel Moisture Database (United States Forest Service, 2018). These maps have low uncertainty across the diverse vegetation and topography of California ($R^2 = 0.63$) and are further described in Text S2, Figures S1 and S2 in Supporting Information S1. We use the most recent pre-lightning LFMC to classify the lightning events.

We use 2016 and 2019 land cover data from the National Land Cover Database (Homer & Fry, 2012), precipitation and VPD data from the Parameter-elevation Regression on Independent Slopes Model (PRISM Climate Group Oregon State University, 2004), elevation data from USGS (2018), canopy height from Simard et al. (2011), NDVI from MODIS (Huete et al., 2010), wind speed from GRIDMET (Abatzoglou, 2011) and the 2010 harmonized AGB map from Spawn et al. (2020). Time-variable and high-resolution AGB datasets do not exist for California; however, we assume spatial variations in AGB dominate temporal variations, and neglect the latter. Because the lightning pairs are also matched on more recent land cover data, and major changes in AGB would be expected to be associated with land cover change, we expect the impact of this assumption to be small.

Because the lightning data has the coarsest spatial resolution of the datasets, we linearly average all other data to that resolution (10 × 10 km), except land cover and fire. For land cover, we assign the most common land cover type to each 10 km grid and filter out the 3.2% of grid cells where it occupies less than 40% of the grid area. For fire, if any 500 m pixel within the lightning footprint burned, we associate that lightning event with an ignition. The data sources and their aggregation are summarized in Table S1 in Supporting Information S1.

3. Results

3.1. Change in Covariate Imbalance After Matching Lightning Strikes

Compared to wet-LFMC lightning strikes, dry-LFMC strikes are biased toward low precipitation, low AGB and dead biomass, shorter vegetation, and high VPD (square points in Figure 2). Multiple covariates (altitude and past VPD) differ by more than one standard deviation between dry-LFMC and wet-LFMC lightning occurrences due to strong cross-correlation with LFMC (Figure S3 in Supporting Information S1), motivating the need to match dry-LFMC and wet-LFMC lightning events to robustly determine the influence of LFMC.

After matching, the standardized difference between the covariates is less than 0.10 for all covariates except VPD (0.30), terrain slope (0.15) and altitude (0.32) (Figure 2). Due to the high bias in dry-LFMC lightning occurrences, we can match only 13,358 out of 38,581 lightning events (Text S1 in Supporting Information S1).

Of the resulting 13,358 lightning events, 235 (or 1.8%) caused an ignition (Figure 3d). Ignition likelihood was strongly correlated to LFMC (correlation = −0.87; Figure S4 in Supporting Information S1). Most of the lightning-caused ignitions are concentrated in northern California, and hence show a different spatial pattern than the strikes without ignitions (Figure 3a). However, we observe no related spatial patterns for the LFMC associated with lightning (Figure 3b), or across land cover types (Figure 3c).

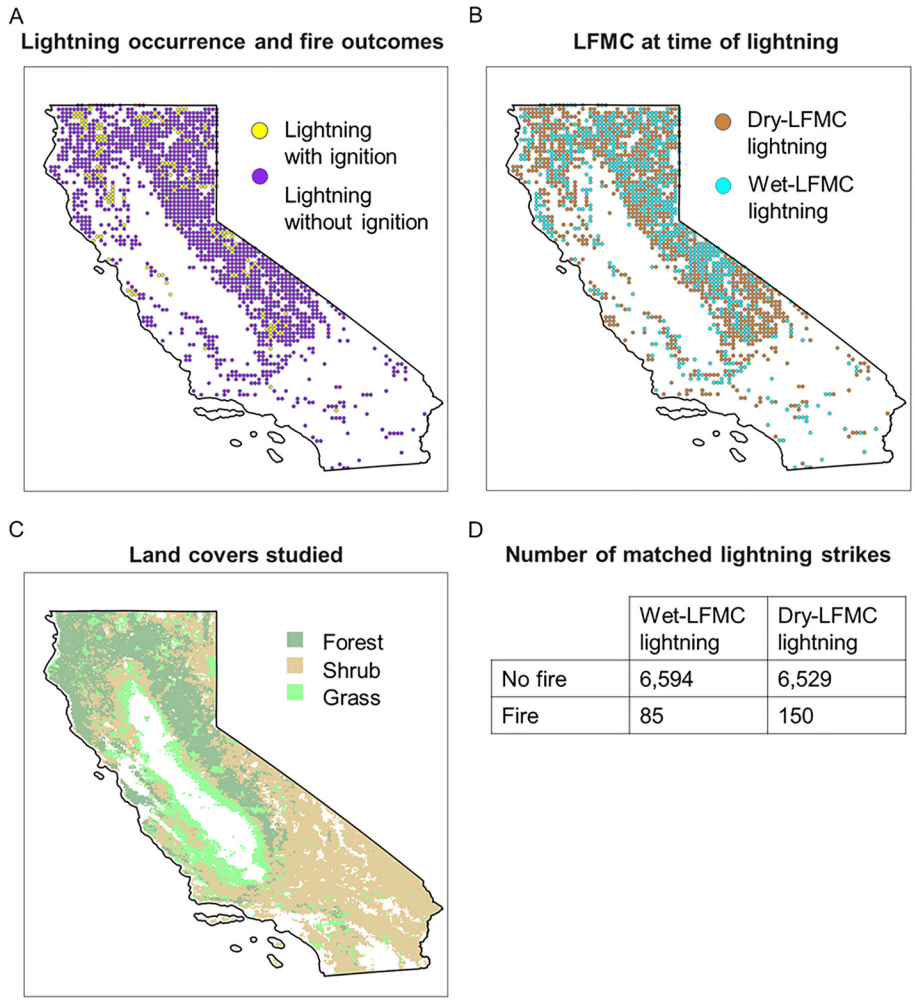

	Wet-LFMC lightning	Dry-LFMC lightning
No fire	6,594	6,529
Fire	85	150

Figure 3. *Lightning, fire, and land properties across the study region.* (a) Yellow (purple) points denote lightning events that ignited (did not ignite) a fire. (b) Brown (cyan) points denote lightning events that struck during dry (wet) Live fuel moisture content conditions. Note that lightning events may overlap. Only lightning events remaining after matching are shown. (c) Land covers included in our analysis. (d) Confusion matrix of lightning events and fire for matched pairs of lightning events.

3.2. Effects of LFMC on Fire Likelihood

Across the 13,358 matched lightning events in our data set, 85 fires ignited in wet-LFMC areas, while 150 fires ignited in dry-LFMC areas. The likelihood of wet-LFMC lightning igniting a fire is thus ∼1-in-78, whereas the likelihood of dry-LFMC lightning igniting a fire is ∼1-in-43. This represents a risk ratio for dry-LFMC lightning of 1.8 (95% confidence interval: 1.4–2.3). That is, when LFMC is less than the land cover-specific threshold—and under constant vegetation, fuel availability and prior meteorology—the likelihood of a fire is 80% higher (Figure 4a). The risk ratio is 2.5 (1.3–4.7) in shrubs, 1.6 (1.2–2.2) in forests, and 1.7 (0.4–6.9) in grasslands. The high uncertainty in grasslands is likely because only 8 out of 235 fires occurred in grasslands.

Segregating the matched pairs of lightning strikes based on their difference in LFMC ($LFMC_{\text{dry-LFMC lightning}} - LFMC_{\text{wet-LFMC lightning}}$) reveals that greater differences in LFMC are associated with a higher likelihood of fire (Figure 4b). The risk ratio is relatively low (1.2; 0.7–1.9) when the difference in LFMC is less than 10% between the matched pairs but exceeds 2.0 when the LFMC differs by more (reaching 2.2 in the highest bin). The risk ratio for all ΔLFMC categories is significant at the 95% confidence level, except when the LFMC difference is less than 10%.

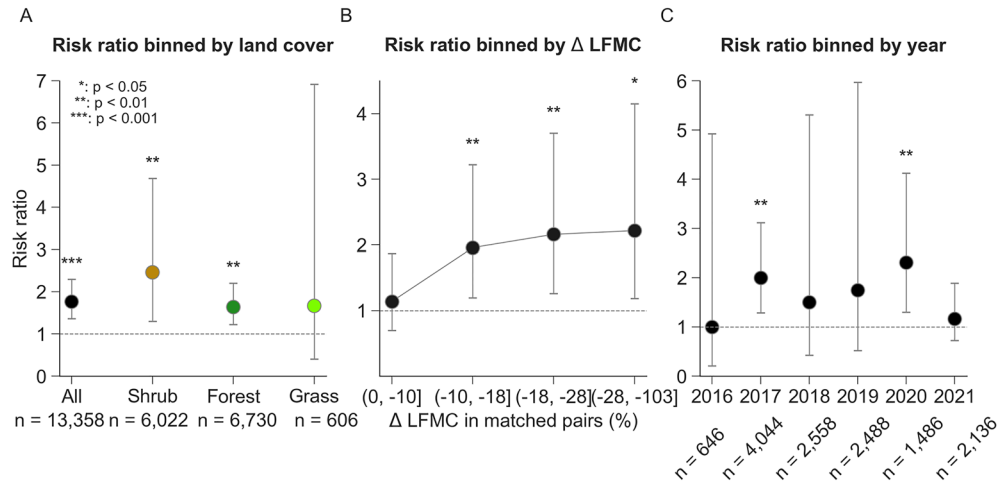

Figure 4. *Risk ratio of dry Live fuel moisture content* (*LFMC*) *causing a fire*. (a) Increased fire likelihood after lightning strikes a region with LFMC < threshold compared to lightning striking a region with LFMC > threshold, either for all pairs (black) or pairs of a specific land cover type (colored). (b) Same as (a), but for lightning pairs segregated by the difference in LFMC between lightning events of each pair. (c) Same as (a), but for lightning pairs segregated by year. For each year, lightning strikes are matched within the respective year only. In all plots, points indicate the mean and whiskers extend to 95% confidence intervals. The dashed line indicates a risk ratio of 1 (no effect).

3.3. Annual Variation in Risk Ratio at Lightning Sites

When compared within years, 2020 had the highest risk ratio (2.3; 1.3–4.1), followed by 2017 (2.0; 1.2–3.1, Figure 4c). All other years' risk ratios are not significant ($p > 0.05$) which may be due to a combination of factors such as where lightning occurs each year, the interannual variability of LFMC, lower sample sizes, etc. (Table S2 and Figure S1 in Supporting Information S1). The risk ratio in 2020 was high even though neither the fraction of dry-LFMC regions (0.7), nor the average difference of LFMC between each matched pair of lightning strikes (−19%) showed significant deviations from other years. Since risk ratios of shrubs and forests differ significantly, we checked for differences in land cover of lightning locations but found that 2020 is not an outlier. However, the lightning strikes leading to ignition in 2020 were overwhelmingly concentrated in August, unlike in other years when the lightning strikes with ignitions were more distributed throughout the warm season (Figure S7 in Supporting Information S1). Note that 2017 also had high risk ratio relative to other years, but did not have an anomalous lightning ignition pattern, nor other clear explanatory patterns in LFMC or land cover to explain the high risk ratio (Table S2 in Supporting Information S1). Further research is needed to explain the high risk ratio in 2017 and more generally, the annual variation of risk ratios.

4. Discussion and Conclusions

Wildfires are complex phenomena that can occur under many conditions, making it difficult to determine the influence of different drivers using correlative studies alone. We provide the first causal evidence that LFMC increases the likelihood of a lightning-caused wildfire after controlling for fuel availability, precipitation, VPD, winds, and other location-specific differences in fuel flammability (Figures 3 and 4). This result is robust in the presence of unobserved confounders (Text S3 and Figure S5 in Supporting Information S1). Thus, under the same fire-weather conditions, LFMC may vary enough to influence live fuel flammability.

The effect of LFMC on ignition risk varies by land cover. The risk ratio is significantly higher for shrubs (2.5) than forests (1.6, Figure 4a), despite the higher LFMC threshold in shrubs. Although few studies have directly measured the lightning ignition efficiency of individual vegetation classes, the available research demonstrates that vegetation composition plays a significant role in lightning fire occurrence. Even outside California, specific conifer species are associated with increased lightning ignition efficiency, leading to high fire occurrences in forests relative to other types of land cover (e.g., Oregon: Díaz-Avalos et al., 2001; Washington: Narayanaraj & Wimberly, 2012; Arizona: Dickson et al., 2006). Vecín-Arias et al. (2016) observed a similar phenomenon on the Iberian Peninsula but noted that the percentage of shrublands within a pixel was positively correlated with

ignition probability due to an abundance of fine fuels. In contrast, in Tasmania, the highest ignition efficiencies were observed in button grass (Nampak et al., 2021). These results further demonstrate that lightning ignition efficiency may vary geographically, as a function of broader climatological and physiological controls.

California's shrubs and forests are located in areas with contrasting climatology and fire-climate regimes (Keeley & Syphard, 2017). Among areas with frequent lightning, shrubs are predominantly located in the high-elevation desert east of the Sierra Nevada, while occupying a higher average elevation than California's forested areas (Figure 3c). As a result, lightning strikes in shrubs have a significantly higher average elevation (Figure S6 in Supporting Information S1) than those in forests, which may influence solar radiation and its effects on live and dead fuel flammability. Further, our LFMC data are derived from a C-band synthetic aperture radar, which does not fully penetrate forest canopies. Because the retrieved LFMC is mostly sensitive to the crown—rather than surface—fuels, LFMC may less accurately reflect the actual live fuels burning in forests (Krawchuk et al., 2006), lowering the apparent influence of LFMC.

Our analysis also sheds light on the role of several factors in driving the record-setting 2020 California fire season, when ~4.3 million acres burned (Safford et al., 2022). 2020 was associated with the highest risk ratio (i.e., high effect of LFMC on ignition probability; Figure 4c), but the risk ratio is not explained by several expected controls. Thus, the higher apparent effect of LFMC on lightning-ignited wildfire must have been promoted by other factors besides those in our framework. Tropical storm Fausto reached California between 15 and 17 August 2020, producing 859 lightning strikes—about 15 times more than the average for any three days between June and November from 2016 to 2021 according to the National Lightning Data Network. Given the unusual concentration of 2020 lightning (Figure S7 in Supporting Information S1), which coincided with an extreme heatwave over California, suppression activities may have been particularly challenged while firefighters attempted to contain large areas simultaneously (Safford et al., 2022). In addition, the COVID-19 pandemic may have challenged suppression efforts in 2020. Although more research is needed to better understand this unusual fire year, our results suggest that human fire management characteristics might modulate how different landscape and climate factors affect natural ignition risk.

Although we report an approximate doubling of the likelihood of a wildfire under dry-LFMC conditions (Figure 4b), fire probability remains low. When LFMC is dry, the probability of a fire given a lightning strike is 2.25%, compared to 1.27% when LFMC is wet (Figure 4d). These low probabilities of lightning ignitions are consistent with previous research (Abatzoglou et al., 2016; Dorph et al., 2022; Nampak et al., 2021).

The improved understanding of LFMC's effect on fuel flammability can be used to inform several fire management practices. LFMC can vary significantly across landscapes and even between nearby species or individuals depending on soil and plant hydraulic traits (Nolan et al., 2022; Rao et al., 2022; Scarff et al., 2021), but these variations are not fully accounted for in fire danger models. Our robust, causal demonstration of the significant role of LFMC in regulating ignition probability motivates further efforts to account for LFMC in wildfire danger estimation, either through using remote sensing-based maps or through ecohydrological models that can forecast spatially variable LFMC responses to weather conditions.

Because California uses a wide network of LFMC measurements (United States Forest Service, 2018) to determine staffing levels of local and regional wildfire response units, a more accurate estimation of LFMC's effect on flammability may improve the allocation of firefighting resources. Similarly, a more accurate quantification of ignition probability can help to target public safety measures, such as power shutoffs to reduce the potential for accidental ignitions. Moreover, there is a severe backlog of prescribed burns in California (Miller et al., 2020). Since the safety of prescribed burns depends partially on LFMC (Biswell, 1999), improved understanding of flammability under different land cover and LFMC conditions may improve prescribed burn planning. As the climate continues to warm and dry, prescribed burn windows may shrink (Dong et al., 2022; Ellis et al., 2021), further fueling the need for an accurate estimate of LFMC's effect on flammability. Finally, as a changing climate alters wildfire regimes in California and globally (Ellis et al., 2021; Keeley & Syphard, 2016) our causal framework may be used to attribute and update the effects of other drivers on wildfire occurrence.

Data Availability Statement

The scripts supporting the analysis can be found at https://doi.org/10.5281/zenodo.8128765. Source of all data used is available in Table S1 in Supporting Information S1.

Acknowledgments
We thank Meng Zhao and three anonymous reviewers for helpful comments on the manuscript. K.R. was funded by the NASA Earth and Space Science Fellowship, and by the Stanford Data Science Scholars Program. A.P.W. was funded by the Zegar Family Foundation and the Moore Foundation. N.S.D acknowledges support from Stanford University. M.Y. acknowledges support from The Australian National University. A.G.K. and K.R. were also funded by the UPS Endowment Fund at Stanford and the Stanford Sustainability Initiative.

References

Abatzoglou, J. T. (2011). Development of gridded surface meteorological data for ecological applications and modelling. *International Journal of Climatology*, *33*(1), 121–131. https://doi.org/10.1002/joc.3413

Abatzoglou, J. T., Battisti, D. S., Williams, A. P., Hansen, W. D., Harvey, B. J., & Kolden, C. A. (2021). Projected increases in western US forest fire despite growing fuel constraints. *Communications Earth & Environment*, *2*(1), 227. https://doi.org/10.1038/s43247-021-00299-0

Abatzoglou, J. T., Kolden, C. A., Balch, J. K., & Bradley, B. A. (2016). Controls on interannual variability in lightning-caused fire activity in the western US. *Environmental Research Letters*, *11*(4), 045005. https://doi.org/10.1088/1748-9326/11/4/045005

Abdollahi, M., Dewan, A., & Hassan, Q. (2019). Applicability of remote sensing-based vegetation water content in modeling lightning-caused forest fire occurrences. *ISPRS International Journal of Geo-Information*, *8*(3), 143. https://doi.org/10.3390/ijgi8030143

Argañaraz, J. P., Landi, M. A., Scavuzzo, C. M., & Bellis, L. M. (2018). Determining fuel moisture thresholds to assess wildfire hazard: A contribution to an operational early warning system. *PLoS One*, *13*(10), 1–19. https://doi.org/10.1371/journal.pone.0204889

Biswell, H. (1999). *Prescribed burning in California wildlands vegetation management - Harold Biswell - Google books*. University of California Press. Retrieved from https://books.google.com/books?hl=en&lr=&id=q6kM12ta8KwC&oi=fnd&pg=PR7&dq=california+prescribed+burns+live+fuel+moisture&ots=7aI8-EnEIf&sig=guIj42Mj1KD4OxxVNdF4xY4oick#v=onepage&q=california%20prescribed%20burns%20live%20fuel%20moisture&f=false

Boschetti, L., Roy, D., Hoffman, A. A., & Humber, M. (2013). Collection 5 MODIS burned area product user guide version 3.0.1. Nasa, Version 1.(May), (pp. 1–12).

Bradshaw, L. S., Deeming, J. E., Burgan, R. E., & Cohen, J. D. (1984). The 1978 national fire-danger rating system: Technical documentation. General Technical Report INT-169. https://doi.org/10.2737/INT-GTR-169

Cal Fire. (2021). Stats & events. Retrieved from https://www.fire.ca.gov/stats-events/

CAL FIRE. (2023). CAL FIRE FRAP historic fire perimeters 2023. Retrieved from https://www.fire.ca.gov/Home/What-We-Do/Fire-Resource-Assessment-Program/GIS-Mapping-and-Data-Analytics

Chang, Y., Zhu, Z., Bu, R., Chen, H., Feng, Y., Li, Y., et al. (2013). Predicting fire occurrence patterns with logistic regression in Heilongjiang Province, China. *Landscape Ecology*, *28*(10), 1989–2004. https://doi.org/10.1007/s10980-013-9935-4

Chuvieco, E., González, I., Verdú, F., Aguado, I., & Yebra, M. (2009). Prediction of fire occurrence from live fuel moisture content measurements in a Mediterranean ecosystem. *International Journal of Wildland Fire*, *18*(4), 430. https://doi.org/10.1071/wf08020

Dadap, N. C., Cobb, A. R., Hoyt, A. M., Harvey, C. F., & Konings, A. G. (2019). Satellite soil moisture observations predict burned area in Southeast Asian peatlands. *Environmental Research Letters*, *14*(9), 094014. https://doi.org/10.1088/1748-9326/ab3891

Dennison, P. E., & Moritz, M. A. (2009). Critical live fuel moisture in chaparral ecosystems: A threshold for fire activity and its relationship to antecedent precipitation. *International Journal of Wildland Fire*, *18*(8), 1021–1027. https://doi.org/10.1071/WF08055

Dennison, P. E., Moritz, M. A., & Taylor, R. S. (2008). Evaluating predictive models of critical live fuel moisture in the Santa Monica Mountains, California. *International Journal of Wildland Fire*, *17*(1), 18–27. https://doi.org/10.1071/wf07017

Díaz-Avalos, C., Peterson, D. L., Alvarado, E., Ferguson, S. A., & Besag, J. E. (2001). Space - time modelling of lightning-caused ignitions in the Blue Mountains, Oregon. *Canadian Journal of Forest Research*, *31*(9), 1579–1593. https://doi.org/10.1139/cjfr-31-9-1579

Dickson, B. G., Prather, J. W., Xu, Y., Hampton, H. M., Aumack, E. N., & Sisk, T. D. (2006). Mapping the probability of large fire occurrence in Northern Arizona, USA. *Landscape Ecology*, *21*(5), 747–761. https://doi.org/10.1007/s10980-005-5475-x

Dong, C., Williams, A. P., Abatzoglou, J. T., Lin, K., Okin, G. S., Gillespie, T. W., et al. (2022). The season for large fires in Southern California is projected to lengthen in a changing climate. *Communications Earth & Environment*, *3*(1), 1–9. https://doi.org/10.1038/s43247-022-00344-6

Dorph, A., Marshall, E., Parkins, K. A., & Penman, T. D. (2022). Modelling ignition probability for human- and lightning-caused wildfires in Victoria, Australia. *Natural Hazards and Earth System Sciences Discussions*, *22*, 1–21. https://doi.org/10.5194/nhess-22-3487-2022

Ellis, T. M., Bowman, D. M. J. S., Jain, P., Flannigan, M. D., & Williamson, G. J. (2021). Global increase in wildfire risk due to climate driven declines in fuel moisture. *Global Change Biology*, *28*, 1–16. https://doi.org/10.1111/gcb.16006

Fernández-Guisuraga, J. M., Suárez-Seoane, S., García-Llamas, P., & Calvo, L. (2021). Vegetation structure parameters determine high burn severity likelihood in different ecosystem types: A case study in a burned Mediterranean landscape. *Journal of Environmental Management*, *288*, 112462. https://doi.org/10.1016/j.jenvman.2021.112462

Fujioka, F. M., Gill, A. M., Viegas, D. X., & Wotton, B. M. (2008). Chapter 21 fire danger and fire behavior modeling systems in Australia, Europe, and North America. *Developments in Environmental Science*, *8*(08), 471–497. https://doi.org/10.1016/S1474-8177(08)00021-1

Goss, M., Swain, D. L., Abatzoglou, J. T., Sarhadi, A., Kolden, C. A., Williams, A. P., & Diffenbaugh, N. S. (2020). Climate change is increasing the likelihood of extreme autumn wildfire conditions across California. *Environmental Research Letters*, *15*(9), 094016. https://doi.org/10.1088/1748-9326/ab83a7

Hardy, C. C., & Hardy, C. E. (2007). Fire danger rating in the United States of America: An evolution since 1916. In *International journal of wildland fire* (Vol. 16, pp. 217–231). Csiro Publishing. https://doi.org/10.1071/WF06076

He, J., Loboda, T. V., Chen, D., & French, N. H. F. (2022). Cloud-to-Ground lightning and near-surface fire weather control wildfire occurrence in Arctic tundra. *Geophysical Research Letters*, *49*(2), 1–11. https://doi.org/10.1029/2021GL096814

Hessilt, T. D., Abatzoglou, J. T., Chen, Y., Randerson, J. T., Scholten, R. C., van der Werf, G., & Veraverbeke, S. (2022). Future increases in lightning ignition efficiency and wildfire occurrence expected from drier fuels in boreal forest ecosystems of western North America. *Environmental Research Letters*, *17*(5), 35. https://doi.org/10.1088/1748-9326/ac6311

Holden, Z. A., & Jolly, W. M. (2011). Modeling topographic influences on fuel moisture and fire danger in complex terrain to improve wildland fire management decision support. *Forest Ecology and Management*, *262*(12), 2133–2141. https://doi.org/10.1016/j.foreco.2011.08.002

Homer, C., & Fry, J. (2012). The national land cover database. US Geological Survey Fact Sheet. Retrieved from http://pubs.usgs.gov/fs/2012/3020/

Huete, A., Didan, K., Leeuwen, W. V., Miura, T., & Glenn, E. (2010). MODIS vegetation indices. In *Land remote sensing and global environmental change* (pp. 579–602). Springer.

Iglesias, V., Balch, J. K., & Travis, W. R. (2022). US fires became larger, more frequent, and more widespread in the 2000s. *Science Advances*, *20*(March), 1–11. https://doi.org/10.1126/sciadv.abc0020

Jurdao, S., Chuvieco, E., & Arevalillo, J. M. (2012). Modelling fire ignition probability from satellite estimates of live fuel moisture content. *Fire Ecology*, *8*(1), 77–97. https://doi.org/10.4996/fireecology.0801077

Keeley, J. E., & Syphard, A. D. (2016). Climate change and future fire regimes: Examples from California. *Geosciences*, *6*(3), 37. MDPI AG. https://doi.org/10.3390/geosciences6030037

Keeley, J. E., & Syphard, A. D. (2017). Different historical fire-climate patterns in California. *International Journal of Wildland Fire*, *26*(4), 253–268. https://doi.org/10.1071/WF16102

Keeley, J. E., & Syphard, A. D. (2019). Twenty-first century California, USA, wildfires: Fuel-dominated vs. wind-dominated fires. *Fire Ecology*, *15*(24), 24. https://doi.org/10.1186/s42408-019-0041-0

Kolden, C. A., & Abatzoglou, J. T. (2018). Spatial distribution of wildfires ignited under katabatic versus non-katabatic winds in Mediterranean Southern California USA. *Fire*, *1*(2), 1–17. https://doi.org/10.3390/fire1020019

Krawchuk, M. A., Cumming, S. G., Flannigan, M. D., & Wein, R. W. (2006). Biotic and abiotic regulation of lightning fire initiation in the mixed wood boreal forest. *Ecology*, *87*(2), 458–468. https://doi.org/10.1890/05-1021

Lund, J., Medellin-Azuara, J., Durand, J., & Stone, K. (2018). Lessons from California's 2012–2016 drought. *Journal of Water Resources Planning and Management*, *144*(10), 04018067. https://doi.org/10.1061/(asce)wr.1943-5452.0000984

Luo, K., Quan, X., He, B., & Yebra, M. (2019). Effects of live fuel moisture content on wildfire occurrence in fire-prone regions over southwest China. *Forests*, *10*(887), 1–17. https://doi.org/10.3390/f10100887

McColl, K. A., Alemohammad, S. H., Akbar, R., Konings, A. G., Yueh, S., & Entekhabi, D. (2017). The global distribution and dynamics of surface soil moisture. *Nature Geoscience*, *10*(2), 100–104. https://doi.org/10.1038/ngeo2868

Miller, R. K., Field, C. B., & Mach, K. J. (2020). Barriers and enablers for prescribed burns for wildfire management in California. *Nature Sustainability*, *3*(2), 101–109. https://doi.org/10.1038/s41893-019-0451-7

Nampak, H., Love, P., Fox-Hughes, P., Watson, C., Aryal, J., & Harris, R. M. B. (2021). Characterizing spatial and temporal variability of lightning activity associated with wildfire over Tasmania, Australia. *Fire*, *4*(1), 1–22. https://doi.org/10.3390/fire4010010

Narayanaraj, G., & Wimberly, M. C. (2012). Influences of forest roads on the spatial patterns of human- and lightning-caused wildfire ignitions. *Applied Geography*, *32*(2), 878–888. https://doi.org/10.1016/j.apgeog.2011.09.004

Nolan, R. H., Boer, M. M., Resco De Dios, V., Caccamo, G., & Bradstock, R. A. (2016). Large-scale, dynamic transformations in fuel moisture drive wildfire activity across southeastern Australia. *Geophysical Research Letters*, *43*(9), 4229–4238. https://doi.org/10.1002/2016GL068614

Nolan, R. H., Foster, B., Griebel, A., Choat, B., Medlyn, B. E., Yebra, M., et al. (2022). Drought-related leaf functional traits control spatial and temporal dynamics of live fuel moisture content. *Agricultural and Forest Meteorology*, *319*, 108941. https://doi.org/10.1016/j.agrformet.2022.108941

Novick, K. A., Ficklin, D. L., Baldocchi, D., Davis, K. J., Ghezzehei, T. A., Konings, A. G., et al. (2022). Confronting the water potential information gap. *Nature Geoscience*, *15*(3), 158–164. https://doi.org/10.1038/s41561-022-00909-2

Orville, R. E., Huffines, G. R., Burrows, W. R., & Cummins, K. L. (2011). The north American lightning detection network (NALDN)-analysis of flash data: 2001-09. *Monthly Weather Review*, *139*(5), 1305–1322. https://doi.org/10.1175/2010MWR3452.1

Pimont, F., Ruffault, J., Martin-StPaul, N. K., & Dupuy, J. L. (2019). Why is the effect of live fuel moisture content on fire rate of spread underestimated in field experiments in shrublands? *International Journal of Wildland Fire*, *28*(2), 127–137. https://doi.org/10.1071/WF18091

Pivovaroff, A. L., Emery, N., Rasoul Sharifi, M., Witter, M., Keeley, J. E., & Rundel, P. W. (2019). The effect of ecophysiological traits on live fuel moisture content. *Fire*, *2*(2), 1–12. https://doi.org/10.3390/fire2020028

PRISM Climate Group Oregon State University. (2004). PRISM climate data.

Quan, X., Yebra, M., Riaño, D., He, B., Lai, G., & Liu, X. (2021). Global fuel moisture content mapping from MODIS. *International Journal of Applied Earth Observation and Geoinformation*, *101*, 102354. https://doi.org/10.1016/j.jag.2021.102354

Rao, K., Williams, A. P., Diffenbaugh, N. S., Yebra, M., & Konings, A. G. (2022). Plant-water sensitivity regulates wildfire vulnerability. *Nature Ecology and Evolution*, *6*(3), 332–339. https://doi.org/10.1038/s41559-021-01654-2

Rao, K., Williams, A. P., Flefil, J. F., & Konings, A. G. (2020). SAR-enhanced mapping of live fuel moisture content. *Remote Sensing of Environment*, *245*, 111797. https://doi.org/10.1016/j.rse.2020.111797

Safford, H. D., Paulson, A. K., Steel, Z. L., Young, D. J. N., Wayman, R. B., & Varner, M. (2022). The 2020 California fire season: A year like no other, a return to the past or a harbinger of the future? *Global Ecology and Biogeography*, *31*, 1–21. https://doi.org/10.1111/geb.13498

Scarff, F. R., Lenz, T., Richards, A. E., Zanne, A. E., Wright, I. J., & Westoby, M. (2021). Effects of plant hydraulic traits on the flammability of live fine canopy fuels. *Functional Ecology*, *35*(4), 835–846. https://doi.org/10.1111/1365-2435.13771

Simard, M., Pinto, N., Fisher, J. B., & Baccini, A. (2011). Mapping forest canopy height globally with spaceborne lidar. *Journal of Geophysical Research*, *116*(4), 1–12. https://doi.org/10.1029/2011JG001708

Spawn, S. A., Sullivan, C. C., Lark, T. J., & Gibbs, H. K. (2020). Harmonized global maps of above and belowground biomass carbon density in the year 2010. *Scientific Data*, *7*(1), 1–22. https://doi.org/10.1038/s41597-020-0444-4

United States Forest Service. (2018). National fuel moisture database. Retrieved from https://www.wfas.net/nfmd/public/index.php

USFS. (2017). Aerial detection and monitoring program. Retrieved from https://www.fs.usda.gov/detail/r5/forest-grasslandhealth/?cid=fsbdev3_046696

USGS. (2018). *USGS EROS archive - digital elevation - global multi-resolution terrain elevation data 2010 (GMTED2010)*. Earth Resources Observation and Science Center. Retrieved from https://www.usgs.gov/centers/eros/science/usgs-eros-archive-digital-elevation-global-multi-resolution-terrain-elevation

Vecín-Arias, D., Castedo-Dorado, F., Ordóñez, C., & Rodríguez-Pérez, J. R. (2016). Biophysical and lightning characteristics drive lightning-induced fire occurrence in the central plateau of the Iberian Peninsula. *Agricultural and Forest Meteorology*, *225*, 36–47. https://doi.org/10.1016/j.agrformet.2016.05.003

Villarreal, M. L., Norman, L. M., Yao, E. H., & Conrad, C. R. (2022). Wildfire probability models calibrated using past human and lightning ignition patterns can inform mitigation of post-fire hydrologic hazards. *Geomatics, Natural Hazards and Risk*, *13*(1), 568–590. https://doi.org/10.1080/19475705.2022.2039787

Westerling, A. L., Hidalgo, H. G., Cayan, D. R., & Swetnam, T. W. (2006). Warming and earlier spring increase western U.S. forest wildfire activity. *Science*, *313*(5789), 940–943. https://doi.org/10.1126/science.1128834

Yebra, M., Dennison, P. E., Chuvieco, E., Riaño, D., Zylstra, P., Hunt, E. R., et al. (2013). A global review of remote sensing of live fuel moisture content for fire danger assessment: Moving towards operational products. *Remote Sensing of Environment*, *136*, 455–468. https://doi.org/10.1016/j.rse.2013.05.029

Yebra, M., Quan, X., Riaño, D., Rozas Larraondo, P., van Dijk, A. I. J. M., & Cary, G. J. (2018). A fuel moisture content and flammability monitoring methodology for continental Australia based on optical remote sensing. *Remote Sensing of Environment*, *212*, 260–272. https://doi.org/10.1016/j.rse.2018.04.053

References From the Supporting Information

Hansen, B. B. (2007). Optmatch: Flexible, optimal matching for observational studies. *R News*, *7*(2), 18–24. Retrieved from http://cran.r-project.org/doc/Rnews/

Rosenbaum, P. R. (2007). Sensitivity analysis for m-estimates, tests, and confidence intervals in matched observational studies. *Biometrics*, *63*(2), 456–464. https://doi.org/10.1111/j.1541-0420.2006.00717.x

USDA. (2017). Aerial detection survey. Retrieved from https://www.fs.usda.gov/detail/r5/forest-grasslandhealth/?cid=fsbdev3_046696